Isovector and isoscalar spin-flip $M1$ strengths in ^{11}B

T. Kawabata,[1,*] H. Akimune,[2] H. Fujimura,[3] H. Fujita,[4] Y. Fujita,[5] M. Fujiwara,[6,7] K. Hara,[8] K. Y. Hara,[2] K. Hatanaka,[6] T. Ishikawa,[9] M. Itoh,[6] J. Kamiya,[10] S. Kishi,[3] M. Nakmura,[11] K. Nakanishi,[6] T. Noro,[12] H. Sakaguchi,[3] Y. Shimbara,[6] H. Takeda,[13] A. Tamii,[6] S. Terashima,[3] H. Toyokawa,[14] M. Uchida,[3] H. Ueno,[13] T. Wakasa,[12] Y. Yasuda,[3] H. P. Yoshida,[6] and M. Yosoi[3]

[1]*Center for Nuclear Study (CNS), University of Tokyo, RIKEN campus, 2-1 Hirosawa, Wako, Saitama 351-0198, Japan*

[2]*Department of Physics, Konan University, Kobe, Hyogo 658-8501, Japan*

[3]*Department of Physics, Kyoto University, Kyoto 606-8502, Japan*

[4]*School of Physics, University of the Witwatersrand, Johannesburg, 2050, South Africa*

[5]*Department of Physics, Osaka University, Toyonaka, Osaka 560-0043, Japan*

[6]*Research Center for Nuclear Physics, Osaka University, Ibaraki, Osaka 567-0017, Japan*

[7]*Advanced Photon Research Center, Japan Atomic Energy Research Institute, Kizu, Kyoto 619-0215, Japan*

[8]*KEK, High Energy Accelerator Research Organization, Tsukuba, Ibaraki 305-0801, Japan*

[9]*Laboratory of Nuclear Science, Tohoku University, Sendai, Miyagi 982-0216, Japan*

[10]*Japan Atomic Energy Institute, Tokai, Ibaraki 319-1195, Japan*

[11]*Wakayama Medical University, Wakayama 641-8509, Japan*

[12]*Department of Physics, Kyushu University, Fukuoka 812-8581, Japan*

[13]*RIKEN (The Institute for Physical and Chemical Research), Wako, Saitama 351-0198, Japan*

[14]*Japan Synchrotron Radiation Research Institute, Hyogo 679-5198, Japan*

The ^{11}B(^{3}He,t), and ^{11}B(d,d'), and ^{11}B(p,p') reactions were measured at forward scattering angles including 0° to study the isovector and isoscalar spin-flip $M1$ strengths in ^{11}B. The measured ^{11}B(^{3}He,t) cross sections were compared with the results of the distorted-wave impulse-approximation (DWIA) calculation, and the Gamow-Teller (GT) strengths for low-lying states in ^{11}C were determined. The GT strengths were converted to the isovector spin-flip $M1$ strengths using the isobaric analog relations under the assumption of the isospin symmetry. The isoscalar spin-flip $M1$ strengths were obtained from the (d,d') analysis by assuming that the shape of the collective transition form factor with the same ΔJ^π is similar in the ^{11}B(d,d') and ^{12}C(d,d') reactions. The obtained isovector and isoscalar strengths were used in the DWIA calculations for the ^{11}B(p,p') reaction. The DWIA calculation reasonably well explains the present ^{11}B(p,p') result. However, the calculated cross section for the 8.92-MeV $3/2_2^-$ state was significantly smaller than the experimental values. The transition strengths obtained in the shell-model calculations were found to be 20–50 % larger than the experimental strengths. The transition strengths for the neutrino induced reactions were estimated by using the isovector and isoscalar spin-flip $M1$ strengths. The present results are quantitatively in agreement with the theoretical estimation discussing the axial isoscalar coupling in the neutrino scattering process, and are useful in the measurement of the stellar neutrinos using the neutral- and charged-current reactions on ^{11}B.

I. INTRODUCTION

The $M1$ transition strengths provide important information to test the validity of theoretical calculations for nuclear structures. Recently, the $M1$ transition strengths are of interest from the view points of not only nuclear physics but also neutrino astrophysics because the spin part of the $M1$ operator is identical with the relevant operators mediating neutrino-induced reactions.

Raghavan *et al.* pointed out that the ^{11}B isotope can be used as a possible neutrino detector to investigate stellar processes [1]. High-energy neutrinos emitted from the stellar processes like the proton-proton fusion chain in the sun and the supernova explosions excite low-lying states in ^{11}B and ^{11}C by $M1$ and Gamow-Teller (GT) transitions via the

neutral-current (NC) and charged-current (CC) processes as seen in Fig. 1. Such neutrinos are detected by measuring emitted electrons from CC reactions and γ rays from the de-excitations of the low-lying states. Since both the NC and CC reactions can be simultaneously measured with one experimental setup using an isospin symmetrical relation between the ^{11}B and ^{11}C, the systematic uncertainty in measuring a ratio of the electron-neutrino flux to the entire neutrino flux is expected to be small. Since the isospin of the ground state of ^{11}B is $T=1/2$, low-lying states in ^{11}B are excited by both the isovector and isoscalar transitions. Therefore, both the isovector and isoscalar responses are needed for estimating the NC cross section. Bernabéu *et al.* estimated the CC and NC cross sections for the several low-lying states in ^{11}B and ^{11}C [2]. They obtained the transition strength for the $1/2_1^-$ state from the available experimental data in a model-independent way. However, the estimations for the other states rely on the shell-model calculation due to the lack of
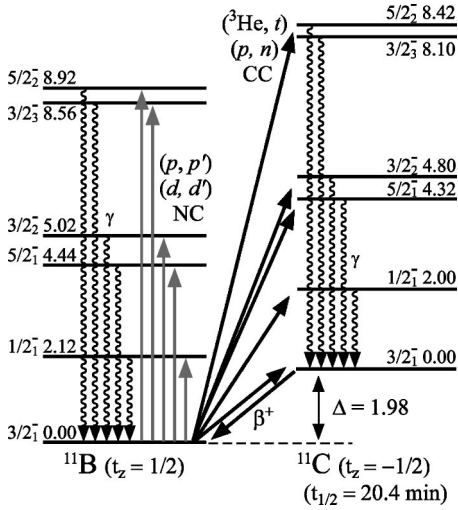
FIG. 1. Level scheme for the low-lying states in ^{11}B and ^{11}C. The states excited by the GT or $M1$ transitions from the ground state of ^{11}B are shown. Energies are given in MeV.

experimental data. Thus, the measurement of the $M1$ strengths for such states in the $A=11$ system is still important.

In addition to the nuclear response, the coupling constants for the weak interaction processes are required for estimating the cross sections of the neutrino-induced reactions. Although the axial isovector coupling constant is well determined as $g_A=1.254\pm0.006$, the axial isoscalar coupling constant f_A remains to be uncertain. The value of f_A directly relates to the strange quark polarization of nucleon. The European Muon Collaboration experiment reported $f_A=0.19\pm0.06$ [3], but another experiment at SLAC presented a smaller value of $f_A=0.12\pm0.02$ [4]. This discrepancy stems from a difficulty in the deep inelastic scattering measurement to cover a small-x region. It is noteworthy that the strange quark polarization and f_A become attainable by measuring neutrino-nucleus inelastic scattering with a neutrino beam if the nuclear response is precisely determined.

The cross sections for hadronic reactions at forward scattering angles have a good proportionality to the relevant transition matrix elements. The cross section for the $(^3\mathrm{He},t)$ reaction can be written in terms of the GT$^-$ operator. On the other hand, the cross section for the (d,d') can be described by the isoscalar $M1$ operator. The cross section for the (p,p') reaction is described by a coherent sum of the isovector and isoscalar $M1$ operators. It is, in principle, possible to obtain the GT and $M1$ strengths by comparing the $(^3\mathrm{He},t)$, (d,d'), and (p,p') cross sections. In this article, we report the results on the GT and $M1$ strengths obtained from three experiments on the $^{11}\mathrm{B}(^3\mathrm{He},t)$, $^{11}\mathrm{B}(d,d')$, and $^{11}\mathrm{B}(p,p')$ reactions.

II. GT AND $M1$ TRANSITION OPERATORS

The GT and $M1$ transition operators are written by

$$\hat{O}(\mathrm{GT}^\pm) = \frac{1}{2}\sum_{k=1}^{A} \boldsymbol{\sigma}_k \tau_\pm(k), \qquad (1)$$

$$\hat{O}(M1) = \left[\sum_{k=1}^{Z} (g_l^\pi \mathbf{l}_k + g_s^\pi \mathbf{s}_k) + \sum_{k=1}^{N} (g_l^\nu \mathbf{l}_k + g_s^\nu \mathbf{s}_k) \right] \mu_N$$

$$= \left[\sum_{k=1}^{A} \left(\frac{g_l^\pi + g_l^\nu}{2} \mathbf{l}_k + \frac{g_s^\pi + g_s^\nu}{2} \frac{\boldsymbol{\sigma}_k}{2} \right) - \left(\frac{g_l^\pi - g_l^\nu}{2} \mathbf{l}_k \right. \right.$$

$$\left. \left. + \frac{g_s^\pi - g_s^\nu}{2} \frac{\boldsymbol{\sigma}_k}{2} \right) \tau_z(k) \right] \mu_N, \qquad (2)$$

where μ_N is the nuclear magneton. For protons and neutrons in the free space, the orbital and spin gyromagnetic factors are $g_l^\pi=1$, $g_l^\nu=0$, $g_s^\pi=5.586$, and $g_s^\nu=-3.826$, respectively. These gyromagnetic factors might be effectively modified in the nuclear medium. The eigenvalues for the isospin operator τ_z are defined as $+1$ for neutrons and -1 for protons. Using the GT and $M1$ transition operators, the GT and $M1$ transition strengths are given by

$$B(\mathrm{GT}^\pm) = \frac{1}{2J_i+1}|\langle f\|\hat{O}(\mathrm{GT}^\pm)\|i\rangle|^2 = \frac{1}{2J_i+1}\left|\frac{1}{2}M(\sigma\tau_\pm)\right|^2,$$

$$(3)$$

$$B(M1) = \frac{1}{2J_i+1}\frac{3}{4\pi}|\langle f\|\hat{O}(M1)\|i\rangle|^2 = \frac{1}{2J_i+1}\frac{3}{4\pi}\left| g_l^{IS} M(l) \right.$$

$$\left. + \frac{g_s^{IS}}{2}M(\sigma) + g_l^{IV}M(l\tau_z) + \frac{g_s^{IV}}{2}M(\sigma\tau_z) \right|^2 \mu_N^2, \qquad (4)$$

where

$$g_{l(s)}^{IS} = \frac{g_{l(s)}^\pi + g_{l(s)}^\nu}{2}, \quad g_{l(s)}^{IV} = \frac{g_{l(s)}^\pi - g_{l(s)}^\nu}{2}, \quad M(\hat{O}) = \langle f\|\hat{O}\|i\rangle.$$

$$(5)$$

J_i is the spin of the initial nuclei. The convention for the reduced matrix elements is according to that of Edmonds [5]. The $M1$ transition strengths consist of the isovector and isoscalar parts, and each of them stems from the orbital and spin contributions. The gyromagnetic factor for the isoscalar spin term is estimated to be $g_s^{IS}=0.880$ from the free-nucleon values, which is much smaller than that for the isovector spin term $g_s^{IV}=-4.706$ in the magnitude. Thus, the isoscalar spin contribution for the $M1$ transition strength is 29 times smaller than the isovector contribution. This means that electromagnetic probes are insensitive to the isoscalar spin part. To obtain the isoscalar spin part, therefore, hadronic probes are useful.

In the case of proton and deuteron scattering off nuclei at forward angles, the spin part of the $M1$ transition strength is dominant. The isovector and isoscalar spin-flip $M1$ strengths are defined by

$$B(\sigma\tau_z) = \frac{1}{2J_i+1}\frac{3}{16\pi}|M(\sigma\tau_z)|^2, \qquad (6)$$

$$B(\sigma) = \frac{1}{2J_i + 1} \frac{3}{16\pi} |M(\sigma)|^2. \qquad (7)$$

There is a simple relation between the isovector spin-flip $M1$ strength and the GT strength for the analog transition to the mirror nucleus under the assumption of the isospin symmetry,

$$\frac{B(\text{GT}^{\pm})}{B(\sigma\tau_z)} = \frac{8\pi}{3} \frac{\langle T_i, T_{iz}, 1, \pm 1 | T_f, T_{fz}\rangle^2}{\langle T_i, T_{iz}, 1, 0 | T_f, T_{fz}\rangle^2}. \qquad (8)$$

Although the isospin-symmetry breaking changes this ratio, the deviation is usually small. Therefore, the GT strengths obtained from the charge exchange reaction are still useful to study the isovector $M1$ strengths.

III. EXPERIMENT

The experiment was performed at the Research Center for Nuclear Physics, Osaka University, using 450-MeV ^{3}He, 200-MeV polarized deuteron, and 392-MeV polarized proton beams. The polarized proton and deuteron beams were obtained from the high-intensity polarized ion source [6]. These beams extracted from the ring cyclotron were achromatically transported to the targets. Although the dispersion matching technique allows us to achieve an extremely better energy resolution [7], the difficulty in obtaining the reliable angular distribution of cross sections is caused due to the large horizontal beam size on targets. The beam intensity on target was in the range of 1–10 pnA. A self-supporting ^{11}B target with a thickness of 16.7 mg/cm^2 and a natural carbon target with a thickness of 30.0 mg/cm^2 were used in the (d,d') measurement. Scattered particles were momentum analyzed by the high-resolution spectrometer Grand Raiden [8]. The focal-plane detector system of Grand Raiden consisting of two multiwire drift chambers and plastic scintillation detectors allowed the reconstruction of the scattering angle at the target via ray-tracing techniques. In the forward angle measurements of the (p,p') and (d,d') reactions, a collimator block was placed in front of the focal plane detectors to avoid a high counting rate due to the elastic scattering events. At extremely forward angles near 0°, the multiple Coulomb scattering caused serious backgrounds. Particles scattered from the target are focused vertically and horizontally at the focal plane of the Grand Raiden spectrometer, while the backgrounds are not focused in the vertical direction. Thus, clean spectra were obtained by subtracting events at the off-median plane from those at the median plane. The detailed explanations have been given in Refs. [9,10]. A focal plane polarimeter (FPP) was used to measure the polarization of protons scattered from the target in the (p,p') reaction. The FPP consisted of a carbon slab with a thickness of 12 cm as a polarization analyzer, four multiwire proportional chambers, and scintillator hodoscopes [11]. For the experimental setup, see Refs. [12,13] and references therein.

Typical spectra of the ^{11}B(^{3}He,t), ^{11}B(p,p'), and ^{11}B(d,d') reactions are shown in Fig. 2. In Figs. 2(b) and 2(c), elastic scattering events disappear since elastically scattered particles were stopped at the collimator block placed in
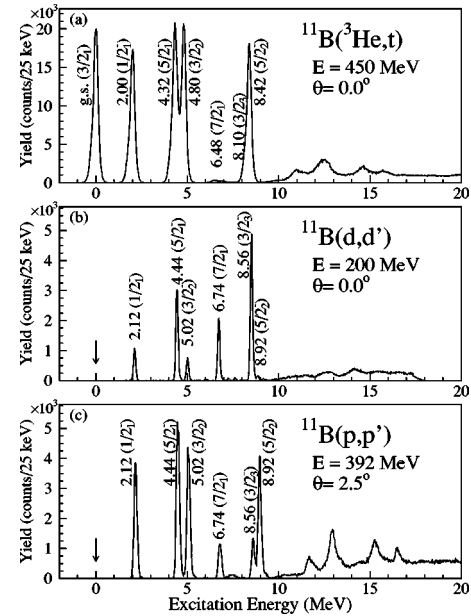

FIG. 2. Typical spectra for the (a) ^{11}B(^{3}He,t), (b) ^{11}B(d,d'), and (c) ^{11}B(p,p') reactions. The peak positions for the elastic deuteron and proton scattering are indicated by the arrows. See text for details.

front of the focal plane detectors. As seen in Fig. 2(b), the excitation-energy spectrum for the ^{11}B(d,d') reaction is observed up to $E_x \simeq 17.5$ MeV. Energy resolutions were determined by fitting the peaks for low-lying states with narrow widths in excitation-energy spectra. An energy resolution of 300 keV full width at half maximum (FWHM) was obtained in the ^{11}B(^{3}He,t) measurement. Since the magnetic spectrometer was operated near the maximum magnetic field in the ^{11}B(^{3}He,t) measurement, the aberration due to the magnetic saturation contributed to deteriorate the energy resolution. In the ^{11}B(d,d') and ^{11}B(p,p') measurements, energy resolutions of 150 and 200 keV (FWHM) were obtained, respectively, which were dominated by the energy spreads of the cyclotron beams. All the prominent peaks were identified as those of known states in ^{11}B or ^{11}C [14]. Contaminating impurities in the ^{11}B target were identified by the kinematic energy shift in the elastic scattering at backward angles, and those contributions were estimated to be less than 1, 0.8, and 0.08 % for ^{10}B, ^{12}C, and ^{16}O, respectively.

IV. RESULT AND DISCUSSION

Since the spin-isospin term $V_{\sigma\tau}$ in the effective interaction is dominant in the (^{3}He,t) reaction at 150 MeV/nucleon, transitions to the strong peaks in Fig. 2(a) are inferred to have a spin-flip nature. On the other hand, the scalar term V_0 is dominant in the (d,d') reaction at 100 MeV/nucleon. Thus, it is natural to infer that the strongly excited states in Fig. 2(b) have a non-spin-flip nature. This simple consideration leads to a qualitative conclusion that the $7/2_1^-$ and $3/2_3^-$ states have a non-spin-flip characteristic while the $5/2_2^-$ state mainly has a spin-flip characteristic.
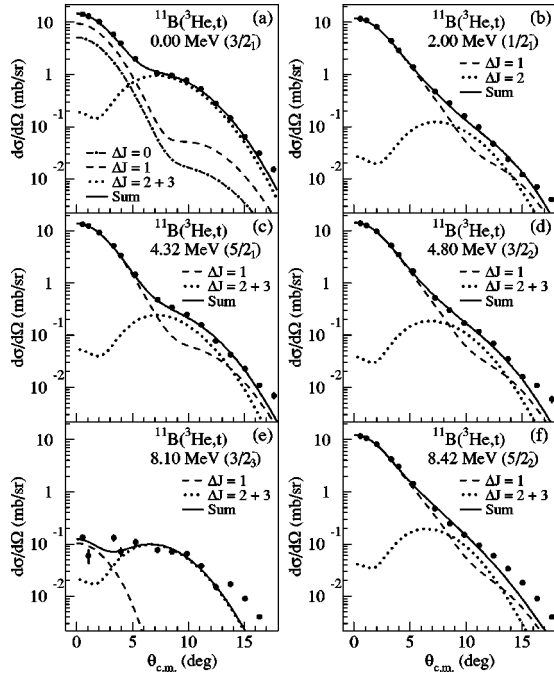
FIG. 3. Cross sections for the ^{11}B(^{3}He,t) reactions compared with the DWIA calculation. The dash-dotted, dashed, and dotted curves show the $\Delta J=0$, $\Delta J=1$, and $\Delta J \geq 2$ contributions, respectively. The solid curves are the sums of all the multipole contributions.

A. ^{11}B(^{3}He,t) reaction

The cross sections for the ^{11}B(^{3}He,t) reaction are shown in Fig. 3. To determine the GT strength from the cross sections, the distorted-wave impulse-approximation (DWIA) calculation was performed using a computer code DWBA98 [15]. Optical-model parameters for the entrance channel were obtained from the ^{3}He elastic scattering on ^{13}C at $E(^3$He$)=450$ MeV [16]. For the exit channel, the same radius and diffuseness with the entrance channel were used while the potential depth was modified to be 85% of the depth for the entrance channel [17]. Wave functions were obtained from the shell-model calculation using the POT interaction by Cohen and Kurath [18]. Single-particle wave

functions were calculated by using a harmonic oscillator (HO) potential, and the oscillation length b for the HO potential was determined for each state to reproduce the measured cross sections as tabulated in Table I.

An effective ^{3}He-N interaction with isospin (V_τ), spin-isospin ($V_{\sigma\tau}$), and isospin-tensor (V_τ^T) terms, represented by a Yukawa potential, was employed to describe the projectile-target interaction. Ranges for the Yukawa potentials were fixed at 1.42 and 0.88 fm for the central and tensor terms, respectively. For the central potential, the strength ratio of $R^2=|V_{\sigma\tau}/V_\tau|^2=8.24\pm0.11$ is widely used at 450 MeV [13], but recent studies implies that a smaller value of R^2 might be preferable for light nuclei [19]. Actually, the R^2 value is estimated to be 5.24 at 150 MeV/nucleon and $A=11$ from the Franey-Love interaction [20]. We, therefore, tested both $R^2=8.24$ and $R^2=5.24$ to study the effect on the final $B(\mathrm{GT}^-)$ values by R^2.

The absolute strength of the central potential was determined by comparing the DWIA calculation with the experimental data for the ground-state transition. The cross section was described by an incoherent sum over the cross sections for the different multipole transitions,

$$\frac{d\sigma}{d\Omega} = \sum_{\Delta J^\pi} A(\Delta J^\pi)\frac{d\sigma}{d\Omega}(\Delta J^\pi), \qquad (9)$$

where the normalization factors $A(\Delta J^\pi)$'s were determined to reproduce the experimental data. Since each multipole cross section was calculated by using shell-model wave functions, the GT and Fermi transition strengths were related to the normalization factors by

$$B(\mathrm{GT}^-)_\mathrm{exp} = A(\Delta J^\pi = 1^+)B(\mathrm{GT}^-)_\mathrm{SM}, \qquad (10)$$

$$B(\mathrm{F})_\mathrm{exp} = A(\Delta J^\pi = 0^+)B(\mathrm{F})_\mathrm{SM}, \qquad (11)$$

where $B(\mathrm{GT}^-)_\mathrm{SM}$ and $B(\mathrm{F})_\mathrm{SM}$ are the GT and Fermi strengths predicted by the shell-model calculation. The ground-state GT transition strength is known to be $B(\mathrm{GT}^-)=0.345\pm0.008$ from the β-decay strength, and the Fermi transition strength is given by $B(\mathrm{F})=N-Z=1$. Since the POT wave function predicted $B(\mathrm{GT}^-)=0.623$ and $B(\mathrm{F})=1.000$ for the ground-state transition, the normalization factors were

TABLE I. Oscillation length used in the DWIA calculation and $B(\mathrm{GT})$ values.

E_x (MeV)	J^π	b (fm)	$B(\mathrm{GT}^-)$[a] $R^2=8.24$	$R^2=5.24$	$B(\mathrm{GT}^-)$[b]
0.00	$3/2^-$	1.61	0.345 ± 0.008		0.345 ± 0.008
2.00	$1/2^-$	1.61	0.402 ± 0.031	0.461 ± 0.036	0.399 ± 0.032
4.32	$5/2^-$	1.66	0.454 ± 0.026	0.521 ± 0.031	$\}\ 0.961\pm0.060$
4.80	$3/2^-$	1.73	0.480 ± 0.031	0.551 ± 0.036	
8.10	$3/2_-$	1.81	≤0.003	≤0.004	$\}\ 0.444\pm0.010$
8.42	$5/2^-$	1.88	0.406 ± 0.038	0.466 ± 0.045	

[a]Present result.
[b]From Ref. [21].

fixed at $A(\Delta J^\pi=1^+)=0.554$ and $A(\Delta J^\pi=0^+)=1.000$ in the analysis. Finally, $V_\tau=1.5$ MeV and $V_{\sigma\tau}=-4.2$ MeV were obtained for $R^2=8.24$ while $V_\tau=1.7$ MeV and $V_{\sigma\tau}=-3.9$ MeV were for $R^2=5.24$. The value of V_τ^T was determined to be -2.5 MeV/fm^2.

The calculated cross sections for the transitions to the ground and excited states in ^{11}C are compared with the experimental results in Fig. 3. Although only the results of the calculations with $R^2=8.24$ are shown in Fig. 3, those of the calculations with $R^2=5.24$ are quite similar. As seen in Fig. 3, the DWIA calculations successfully explain the experimental results. It is noted that the $\Delta J^\pi=1^+$ excitations dominate the cross sections for all the negative parity states in Fig. 3 except the 8.10-MeV $3/2_3^-$ state due to the large R^2 value.

The GT strengths obtained from the $\Delta J^\pi=1^+$ cross sections are compared with the previous (p,n) result [21] in Table I. The present results are consistent with the (p,n) result although several states are not resolved in the (p,n) measurement due to poor energy resolution. We found that the $R^2=8.24$ results give the $B(\mathrm{GT}^-)$ values close to the (p,n) result. The $B(\mathrm{GT}^-)$ values for $R^2=8.24$ are smaller than those for $R^2=5.24$ by 15%. This difference of 15% in the $B(\mathrm{GT}^-)$ values almost equals to the difference in the $|V_{\sigma\tau}|^2$ values between the $R^2=8.24$ and 5.24 cases. This fact indicates that the factorized expression for the charge exchange reaction [22] gives a good description for the $(^3\mathrm{He},t)$ reaction at $E(^3\mathrm{He})=450$ MeV. Since the $B(\mathrm{GT}^-)$ value for the $3/2_3^-$ state is very small, we could only give the upper limit. This small $B(\mathrm{GT}^-)$ value is consistent with the previous simple consideration that the $3/2_3^-$ state has a non-spin-flip characteristic.

B. ^{11}B(d,d') and ^{12}C(d,d') reactions

The measured cross sections for the ^{11}B(d,d') and ^{12}C(d,d') reactions exciting the several low-lying states are shown in Figs. 4 and 5. The (d,d') cross section was given by an incoherent sum over the cross sections for the different multipole transitions. To derive the isoscalar spin-flip $M1$ strength $B(\sigma)$ from the experiment, the (d,d') cross section for each ΔJ^π transition was needed.

Microscopic calculations for deuteron induced reactions are generally difficult because the deuteron is a loosely bound two-body system and its internal degree of freedom has to be taken into account. Recently, a microscopic calculation using a three-body d-N interaction was performed and gave a good description for the ^{12}C(d,d') reaction at $E_d=270$ MeV at backward angles of $\theta \gtrsim 5°$ [23]. This calculation, however, does not reproduce the angular distribution of the cross section at forward angles near $0°$ where $\Delta J^\pi=1^+$ transitions become strong. Therefore, the application of such microscopic calculations is not suitable for our purpose to estimate the cross sections for each ΔJ^π transition and to determine the isoscalar spin-flip $M1$ strength. In the present work, we measured the ^{12}C(d,d') reaction for the comparison with the ^{11}B(d,d') reaction. Since the spin-parity of the ground state of ^{12}C is 0^+, transitions to the discrete states in
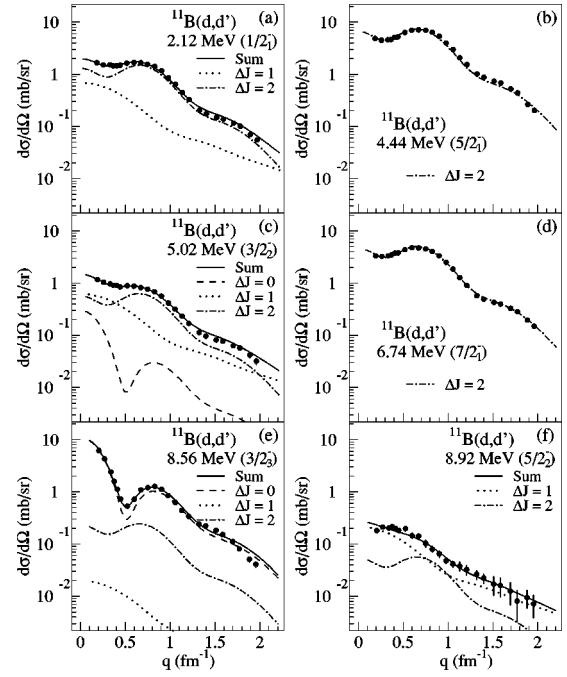

FIG. 4. Cross sections for the nonparity changing transitions in deuteron inelastic scattering on ^{11}B. The dashed, dotted, and dash-dotted curves show the $\Delta J=0$, 1, and 2 contributions, respectively. The solid curves are the sums of all the multipole contributions.

^{12}C are expected to be good references for the angular distributions of the cross sections for certain ΔJ^π transitions.

To parametrize the angular distributions of the cross sections for the 4.44-MeV 2_1^+ and 7.65-MeV 0_2^+ states in ^{12}C, we asked for a help of a deformed potential (DP) model calculation using a computer code ECIS95 [24]. Optical-model potentials for the DP-model analysis were parametrized as

$$U(r)=-Vf(r,r_R,a_R)-iWf(r,r_I,a_I)$$
$$+2\left(\frac{\hbar}{m_\pi c}\right)^2 V_{SO}\frac{1}{r}\frac{d}{dr}f(r,r_{SO},a_{SO})\boldsymbol{l}\cdot\boldsymbol{s}+V_C, \quad (12)$$

where

$$f(r,r_x,a_x)=\left[1+\exp\left(\frac{r-r_xA^{1/3}}{a_x}\right)\right]^{-1}. \quad (13)$$

The Coulomb potential V_C was taken as that of a uniformly charged sphere with a radius of $R_C=1.3A^{1/3}$ fm. Three parameter sets B, C, and BC tabulated in Table II were determined by fitting the cross sections, vector analyzing powers (A_y), and tensor analyzing powers (A_{yy}) for the elastic scattering from the ^{11}B and ^{12}C targets. The parameter sets B and C were obtained from the independent analysis of the ^{11}B and ^{12}C data. The parameter set BC was determined by fitting both the ^{11}B and ^{12}C data simultaneously. As seen from the χ^2 values in Table II, almost the same quality of the fit is obtained for the three parameter sets. The results from the optical-model calculation with the parameter set BC are presented by the solid lines in Fig. 6.

Using the obtained optical-model potential, we calculated the transition potential according to the prescription of the
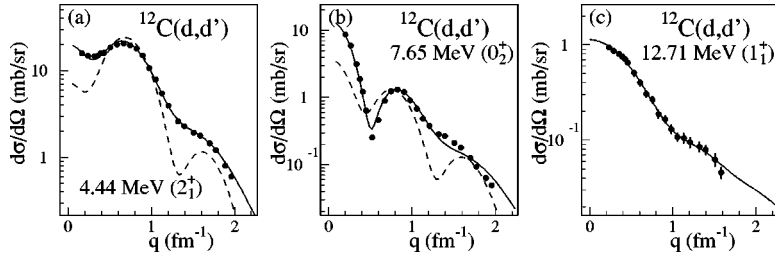
FIG. 5. Cross sections for the nonparity changing transitions in deuteron inelastic scattering on ^{12}C.

DP model [25]. The result of the DP-model calculation with the parameter set BC is shown by the dashed lines in Figs. 5(a) and 5(b). Unfortunately the DP-model calculation with the parameter set BC is not satisfactory for reproducing the cross sections for the 2_1^+ and 0_2^+ states. To obtain the better descriptions, we modified the optical-model potentials by fitting the elastic and inelastic scattering data simultaneously. During the process of the modification, the potential parameters for the $\Delta J^\pi = 0^+$ and 2^+ transitions were searched for independently, and we additionally introduced the real and imaginary surface terms into the optical-model potential. This procedure means that we allocate additional degrees of freedom for the precise parametrization of the potential shape in the surface region where the incident deuterons are strongly absorbed. As the result of the modification, the $\Delta J^\pi = 2^+$ and 0^+ cross sections were well-fitted as shown by the solid lines in Figs. 5(a) and 5(b) although the optical-model calculations for the elastic scattering became slightly worse as seen in Fig. 6. We estimated that the change of the cross-section values due to the coupled channel effect is smaller than 10%. This effect is, therefore, neglected in the present analysis.

Although a question is addressed on the physical interpretation of the potential modification described above, it should be emphasized that our purpose is simply to parametrize the angular distributions of the cross section for the $\Delta J^\pi = 0^+$ and 2^+ transitions in the ^{12}C(d,d') reaction and to perform the multipole decomposition analysis for the ^{11}B(d,d') reaction. The basic assumption of the present analysis is that the collective transition form factors reflected to the cross-section shape for a certain ΔJ^π transition in the ^{12}C(d,d') and ^{11}B(d,d') reactions are similar. The validity of this assumption could be tested by checking whether the angular distribution in the ^{11}B(d,d') reaction is reasonably explained or not.

On the other hand, the angular distribution of the cross section for the 12.71-MeV 1_1^+ state was parametrized as a function of the momentum transfer q using spherical Bessel functions

$$\frac{d\sigma}{d\Omega}(1_1^+) = \alpha_0 |j_0(qR_0)|^2 + \alpha_2 |j_2(qR_2)|^2. \tag{14}$$

Four parameters in the above equation were determined to be $R_0 = 1.26A^{1/3}$ fm, $R_1 = 1.52A^{1/3}$ fm, $\alpha_0 = 1.13$ mb/sr, and $\alpha_1 = 1.27$ mb/sr by fitting the experimental data as shown by the solid line in Fig. 5(c).

The cross sections for the $\Delta J^\pi = 0^+$, 1^+, and 2^+ transitions in the ^{11}B(d,d') reaction were calculated using the modified potentials for the DP-model calculation and the spherical Bessel functions which were determined in the ^{12}C(d,d') analysis. Then, the measured ^{11}B(d,d') cross sections were fitted by combining the calculated cross sections. In the fitting procedure, the higher multipole contributions with $\Delta J \geq 3$ were neglected. As seen in Fig. 4, the experimental results were well reproduced in the fit. This means that the basic assumption on the similarity between the ^{12}C(d,d') and ^{11}B(d,d') reactions is reasonable.

Although the 4.44-MeV $5/2_1^-$ state can be excited by both the $\Delta J^\pi = 1^+$ and 2^+ transitions, the main part of the transition is due to $\Delta J^\pi = 2^+$. This result is explained if the ground and 4.44-MeV states are the strongly coupled members of the ground-state rotational band. Since the observed $\Delta J^\pi = 2^+$ transition strength is much stronger than the expected $\Delta J^\pi = 1^+$ strength, the $\Delta J^\pi = 1^+$ component of the transition strength can not be reliably extracted for the 4.44-MeV state. The transition strength for the 6.74-MeV $7/2_1^-$ state is also dominated by the $\Delta J^\pi = 2^+$ component although the $\Delta J^\pi = 1$ transition to this state is not allowed.

The cross section for the $\Delta J^\pi = 1^+$ transition is known to be proportional to the isoscalar spin-flip $M1$ strength $B(\sigma)$. The $B(\sigma)$ value for the transition to the 2.12-MeV $1/2_1^-$ state is 0.037 ± 0.008, which is obtained from the γ-decay widths of the mirror states and the $B(\text{GT}^-)$ value [2]. Using this value, the cross sections for the $\Delta J^\pi = 1^+$ transitions for other excited states were converted to the $B(\sigma)$ values as tabulated in Table III. Systematic uncertainties on $B(\sigma)$ are mainly due to errors in the model calculation for the (d,d') reaction. The

TABLE II. Optical model parameters derived from our best fit to the elastic scattering data. Parameter sets B and C were determined by fitting the elastic scattering on ^{11}B and ^{12}C, respectively, while BC was by fitting both the ^{11}B and ^{12}C data simultaneously.

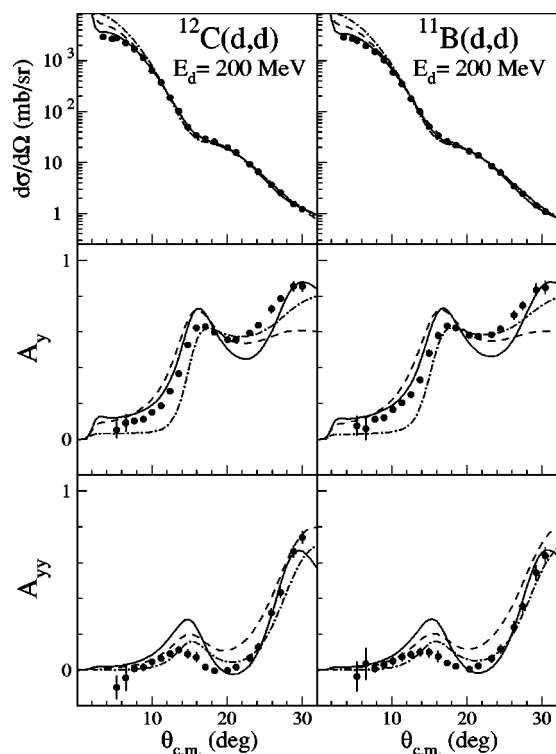|	V (MeV)	r_R (fm)	a_R (fm)	W (MeV)	r_I (fm)	a_I (fm)	V_{SO} (MeV)	r_{SO} (fm)	a_{SO} (fm)	χ^2
B	20.36	1.50	0.65	35.25	0.66	1.06	1.68	1.00	0.68	1160
C	20.45	1.51	0.65	31.45	0.78	1.02	1.79	0.98	0.70	1396
BC	20.24	1.51	0.65	33.27	0.72	1.05	1.74	0.99	0.69	2599

FIG. 6. Cross sections, vector analyzing powers A_y, and tensor analyzing powers A_{yy} for the deuteron elastic scattering on ^{12}C and ^{11}B compared with the results of the optical-model calculations. The solid lines show the results with the parameter set BC. The dashed and dash-dotted lines show the results using the modified optical-model potentials for the $\Delta J^\pi = 0^+$ and 2^+ transitions, respectively.
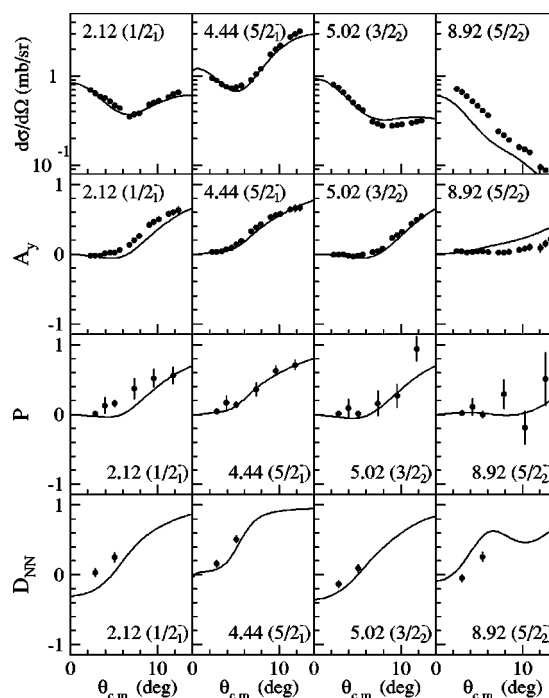

FIG. 7. Cross sections, vector analyzing powers A_y, induced polarizations P, and depolarization parameters D_{NN} for the ^{11}B(p,p') reaction compared with the results of the DWIA calculations.

normalization uncertainty of 20% is not shown in Table III, which is attributed to the uncertainty on the $B(\sigma)$ value for the 2.12-MeV state taken from Ref. [2].

The 8.56-MeV $3/2_3^-$ state, which is not predicted by the shell-model calculation with the POT potential, has a strong $\Delta J^\pi = 0^+$ component. Although the isobaric analog state of the 8.56-MeV state is observed at $E_x = 8.10$ MeV in the ^{11}B$(^3$He$,t)$ reaction, the excitation strength is extremely weak. These facts indicate that the $3/2_3^-$ state in the $A = 11$ system is collective, and the single-particle aspect of its wave function is small.

TABLE III. Isoscalar spin-flip $M1$ transition strength $B(\sigma)$. Systematic uncertainties are mainly due to errors in the DP model calculations. The normalization uncertainty of 20% attributed to the uncertainty on the calibration reference is not shown.

E_x (MeV)	J^π	$B(\sigma)$
2.12	$1/2_1^-$	0.037 ± 0.007[a]
4.44	$5/2_1^-$	–
5.02	$3/2_2^-$	0.035 ± 0.005
8.56	$3/2_3^-$	$\leqslant 0.003$
8.92	$5/2_2^-$	0.012 ± 0.003

[a]From Ref. [2].

C. ^{11}B(p,p') reaction

The cross sections, analyzing powers (A_y), induced polarizations (P), and depolarization parameters (D_{NN}) for the ^{11}B(p,p') reaction are shown in Fig. 7. The DWIA calculation was performed by using the computer code DWBA98. The effective nucleon-nucleon interaction derived by Franey and Love at 425 MeV [20] was used in the calculations. The global Dirac optical-model potential was used in the Schrödinger equivalent form [26] to give the distorted waves of incoming and outgoing protons. The (p,p') cross sections were given by an incoherent sum over the cross section of the different multipole contribution as in $(^3$He$,t)$ and (d,d') reactions. The cross section for each ΔJ^π transition was described by a coherent sum of the isovector and isoscalar contributions.

Since the isovector and isoscalar transition strengths for the several states in ^{11}B have been already obtained from the $(^3$He$,t)$ and (d,d') analyses in the present work, the DWIA calculation for the ^{11}B(p,p') reaction can be performed without any free parameters. The isovector strengths determined by using $R^2 = 8.24$ were used in the calculation. Since the isoscalar spin-flip $M1$ strength was not reliably determined in the (d,d') analysis for the 4.44-MeV state, the isoscalar spin-flip $M1$ strength was assumed to be

$$B(\sigma)_{\text{exp}} = B(\sigma\tau_z)_{\text{exp}} \frac{B(\sigma)_{\text{SM}}}{B(\sigma\tau_z)_{\text{SM}}}, \quad (15)$$

i.e., the relative strength of the isoscalar transition to the isovector transition was taken from the the shell-model calculation.

As shown in Fig. 7, the DWIA calculation well explains the experimental results except the cross section for the transition to the 8.92-MeV state. This supports the reliability of the ^{11}B(^{3}He, t) and ^{11}B(d, d') analyses. The calculated cross section for the 8.92-MeV state is about 50% smaller than the experiment. One remarkable fact predicted by the DWIA calculation using the POT wave functions is that the isovector and isoscalar components destructively contribute for the $\Delta J^\pi = 1^+$ transition to the 8.92-MeV state, while these two components constructively contribute for the 2.21-MeV, 4.44-MeV, and 5.02-MeV states. However, the considerable decrease of 50% in the (p, p') cross section cannot be explained even if a constructive interference is assumed. The reason why the DWIA calculation underestimates the cross section for the transition to the 8.92-MeV state is still unclear. The result may imply that the 8.92-MeV state has a wave function totally different from the other states at 2.12, 4.44, and 5.02 MeV.

Since the $|V_{\sigma\tau}/V_\sigma|^2$ value of the effective nucleon-nucleon interaction is large, the cross section for the $\Delta J^\pi = 1^+$ transition is dominated by the isovector component and is insensitive to the relative strength between the isovector and isoscalar components. However, the polarization transfer observables are sensitive to the relative strength in the spin-flip transition. Since the depolarization parameter was measured in the present experiment, the relative strength between the isovector and isoscalar components in the $\Delta J^\pi = 1^+$ transition is, in principle, determined from the (p, p') result. Although we tried to determine the relative strength by fitting the measured depolarization parameter, such analyses were found to be unacceptable; the isoscalar strengths for all the states are strongly suppressed. This unrealistic result is mainly caused by errors in the effective nucleon-nucleon interaction. Therefore, the precise determination of the effective interaction is strongly desired. Additional measurements of other kinds of the polarization transfer observables (e.g., D_{SS} and D_{LL}) would be helpful in clarifying the unclear situation discussed above.

D. Comparisons with the previous experiment and the shell-model calculation

Although the two doublets at 4.32–4.80 MeV and 8.11–8.42 MeV in ^{11}C are not separately resolved in the previous (p, n) measurement [21], the $B(\text{GT}^-)$ values for the charge exchange reactions to the low-lying states in ^{11}C have been obtained. Recently, the $B(\sigma\tau_z)$ values for the low-lying states in ^{11}B are reported by KVI group from the (p, p') measurement at $E_p = 150$ MeV [27]. These results are compared with the present results in Fig. 8. The result with $R^2 = 8.24$ is preferable from a view of the consistency with the (p, n) results. The results from Ref. [27] are systematically smaller than those from the other experiments. This inconsistency seems to be originated from the difficult normalization process in the DWIA calculation. The calculated cross sections depend on various parameters, i.e., the nuclear transition strength, the distorting potential, the effective interaction, and so on. The uncertainties of the distorting potential
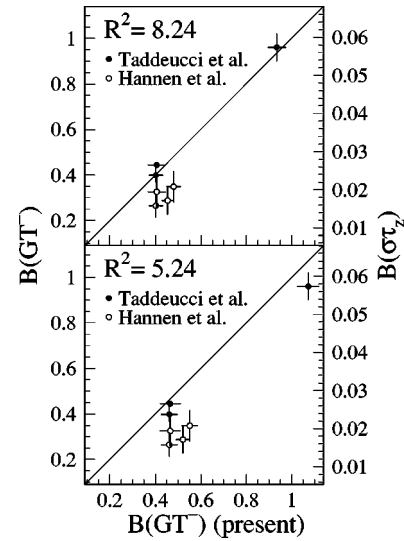

FIG. 8. $B(\text{GT}^-)$ from Ref. [21] (solid circles) and $B(\sigma\tau_z)$ from Ref. [27] (open circles) are compared with the present results in the cases of $R^2 = 8.24$ (upper panel) and $R^2 = 5.24$ (lower panel). The horizontal axis indicates the $B(\text{GT}^-)$ values from the present study and the vertical axis shows the $B(\text{GT}^-)$ or $B(\sigma\tau_z)$ values from the previous experiments. The solid lines are drawn to guide the eye.

and the effective interaction cause large systematic uncertainties in the normalization.

The present results are compared with the shell-model predictions using the POT [18] and SFO (Suzuki-Fujimoto-Otsuka) [28] interactions in Fig. 9. The shell-model calculations with the POT and SFO interactions are performed in the $0\hbar\omega$ and 0–$2\hbar\omega$ configuration spaces, respectively. The hatched and open bars in the left panels show the $B(\text{GT}^-)$ results deduced from the analyses using $R^2 = 8.24$ and $R^2 = 5.24$, respectively. The open bar in the upper-right panel shows the $B(\sigma)$ value for the 4.44-MeV state, which is estimated from the $B(\text{GT}^-)$ value by using Eqs. (8) and (15). Both the calculations with the POT and SFO wave functions
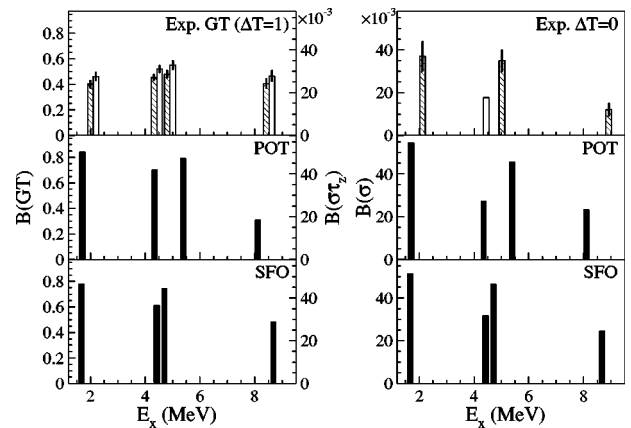

FIG. 9. Measured $B(\text{GT}^-)$ [$B(\sigma\tau_z)$] and $B(\sigma)$ values are compared with the shell-model predictions using the POT [18] and SFO [28] interactions. The hatched and open bars in the left panels show the $B(\text{GT})$ results deduced by using $R^2 = 8.24$ and $R^2 = 5.24$, respectively. The open bar in the right panel shows the $B(\sigma)$ value for the 4.44-MeV state estimated from $B(\text{GT})$ (see text).

TABLE IV. Transition strengths in the unit of g_A^2 for the neutrino induced reactions via the neutral-current process in ^{11}B. $f_A = 0$ is assumed in Refs. [27] and [29].

J^π	λ_{NC}/g_A^2			
	Present	Ref. [2]	Ref. [27]	Ref. [29]
$1/2_1^-$	$0.101(8)[1+1.3(f_A/g_A)]^2$	$0.100[1+1.3(f_A/g_A)]^2$	0.068(13)	0.089(6)
$5/2_1^-$	$0.114(7)[1+0.8(f_A/g_A)]^2$	$0.114[1+1.0(f_A/g_A)]^2$	0.073(15)	0.146(14)
$3/2_2^-$	$0.120(8)[1+1.1(f_A/g_A)]^2$	$0.127[1+1.2(f_A/g_A)]^2$	0.088(18)	0.146(6)
$5/2_2^-$	$0.102(10)[1-0.7(f_A/g_A)]^2$		0.083(18)	

well explain the excitation energies, but the predicted excitation strengths are unacceptably large. The calculations with the SFO wave functions are better in describing the excitation strength since the $2p$-$2h$ configuration mixing is taken into account, but the excitation strengths are still overestimated by 20–50 %.

E. Transition strengths for neutrino induced reactions

The cross section for the CC transition ^{11}B(ν_e,e^-) is given as follows at the long wavelength limit [2],

$$\sigma_{CC} = \frac{(G_F \cos\theta_c)^2}{4\pi} \frac{1}{2J_i+1}[|M(\tau_-)|^2$$
$$+ g_A^2|M(\sigma\tau_-)|^2]E_e'|\mathbf{p}_e'|F(Z,E_e'), \quad (16)$$

where G_F is the Fermi coupling constant, θ_c is the Cabibbo angle, g_A is the axial isovector coupling constant, J_i is the initial nuclear spin, E_e' ($\mathbf{p}_e'$) is the energy (momentum) of the outgoing electron, $F(Z,E_e')$ is the Coulomb function for the final electron, and Z is the charge of the residual nucleus. The cross section for the NC transition ^{11}B(ν_x,ν_x') is

$$\sigma_{NC} = \frac{(G_F E')^2}{4\pi} \frac{1}{2J_i+1}|f_A M(\sigma) + g_A M(\sigma\tau_z)|^2, \quad (17)$$

where f_A and E' are the axial isoscalar coupling constant and outgoing neutrino energy, respectively. The nuclear structural parts of the cross section formulae are summarized by

$$\lambda_{CC} = \frac{1}{4(2J_i+1)}[|M(\tau_-)|^2 + g_A^2|M(\sigma\tau_-)|^2] = B(\text{F}) + g_A^2 B(\text{GT}^-)$$
$$(18)$$

$$\lambda_{NC} = \frac{1}{4(2J_i+1)}|f_A M(\sigma) + g_A M(\sigma\tau_z)|^2. \quad (19)$$

The λ_{NC} values determined from the present $B(\text{GT}^-)$ ($R^2 = 8.24$) and $B(\sigma)$ values are compared with the estimations in the several works [2,27,29] in Table IV. The isovector and isoscalar components destructively contribute to λ_{NC} for the $5/2_2^-$ state although they constructively contribute for the other states. The relative phases between the isovector and isoscalar components were taken from the shell-model predictions, which are in agreement with the results of the ^{11}B(p,p') analyses for the $1/2_1^-$, $5/2_1^-$, and $3/2_2^-$ states in ^{11}B.

The value of f_A/g_A is known to be 0.1–0.15 from the experiments [3,4], meaning that the contribution from the axial isoscalar coupling to the NC process increases the expected NC strength by 40%. It is noted that the isoscalar contributions were neglected in Refs. [27,29].

In Ref. [2], the λ_{NC} value for the $1/2_1^-$ state was determined from the experimental data without using any particular nuclear model, but those for the other states were estimated by combining the results from the experiments and from the shell-model calculation. The estimated λ_{NC} values given in Ref. [2] are consistent with the present experimental result.

V. SUMMARY

We measured cross sections for the ^{11}B$(^3\text{He},t)$, ^{11}B(d,d'), and ^{11}B(p,p') reactions at forward scattering angles including 0° to study the isovector and isoscalar spin-flip $M1$ transition strengths. Analyzing powers, induced polarizations, and depolarization parameters were measured for the ^{11}B(p,p') reaction.

The measured ^{11}B$(^3\text{He},t)$ cross sections were compared with the DWIA calculation using the POT wave functions. The effective ^{3}He-N interaction was obtained by fitting the cross sections for the ground-state transition. The cross sections for the transitions to the excited states in ^{11}C were decomposed into each ΔJ^π component based on the DWIA calculation, and the $B(\text{GT}^-)$ values were extracted from the $\Delta J^\pi = 1^+$ contribution. The $B(\text{GT}^-)$ values are easily converted to the isovector spin-flip $M1$ strengths $B(\sigma\tau_z)$ for the analog transitions under the assumption of the isospin symmetry.

In the analysis of the ^{11}B(d,d') reaction, we used the ^{12}C(d,d') reaction as a measure to obtain the angular distribution of the cross section for each ΔJ^π contribution. After the angular distribution was obtained, the ^{11}B(d,d') cross section for each excited state was decomposed into the $\Delta J^\pi = 0^+$, 1^+, and 2^+ components. Finally, the obtained cross section for the $\Delta J^\pi = 1^+$ component was converted to the isoscalar spin-flip $M1$ strength $B(\sigma)$.

The isovector and isoscalar transition strengths obtained in the ^{11}B$(^3\text{He},t)$ and ^{11}B(d,d') analyses were used for performing the DWIA calculation to analyze the ^{11}B(p,p') reaction data. The DWIA calculation reasonably explains the present ^{11}B(p,p') result except the cross section for the transition to the 8.92-MeV states and supports the reliability of

the present ^{11}B(^{3}He, t) and ^{11}B(d, d') analyses. The DWIA calculation considerably underestimates the cross section for the transition to the 8.92-MeV state. This result implies that the 8.92-MeV state has a nature totally different from the other three states at the lower excited energies.

The obtained spin-flip $M1$ strengths were compared with the shell-model calculations using the POT and SFO interactions. Although the excitation energies for the excited states are reasonably in agreement with the shell-model calculations, the transition strengths are overestimated by 20–50 %. The transition strengths for the neutrino induced reactions were estimated by using the isovector and isoscalar spin-flip $M1$ strengths. The present results are quantitatively in agreement with the theoretical estimation discussing the axial-isoscalar coupling in the neutrino scattering process, and are

useful in the future measurement of the stellar neutrinos using the neutral- and charged-current reactions on ^{11}B.

[1] R. Raghavan, S. Pakvasa, and B. Brown, Phys. Rev. Lett. **57**, 1801 (1986).

[2] J. Bernabéu, T. Ericson, E. Hernández, and J. Ros, Nucl. Phys. **B378**, 131 (1992).

[3] European Muon Collaboration, J. Ashman *et al.*, Nucl. Phys. **B328**, 1 (1989).

[4] E155 Collaboration, P. Anthony *et al.*, Phys. Lett. B **493**, 19 (2000).

[5] A. Edmonds, *Angular Momentum in Quantum Mechanics* (Princeton University Press, Princeton, NJ, 1960).

[6] K. Hatanaka, K. Takahisa, H. Tamura, M. Sato, and I. Miura, Nucl. Instrum. Methods Phys. Res. A **384**, 575 (1997).

[7] T. Wakasa *et al.*, Nucl. Instrum. Methods Phys. Res. A **482**, 79 (2002).

[8] M. Fujiwara *et al.*, Nucl. Instrum. Methods Phys. Res. A **422**, 484 (1999).

[9] M. Itoh *et al.*, Phys. Rev. C **68**, 064602 (2003).

[10] M. Uchida *et al.*, Phys. Lett. B **557**, 12 (2003).

[11] M. Yosoi *et al.*, in *High Energy Spin Physics*, edited by K. J. Heller and S. L. Smith, AIP Conf. Proc. No. 343, (AIP, New York, 1995), p. 157.

[12] T. Kawabata *et al.*, Phys. Rev. C **65**, 064316 (2002).

[13] H. Akimune *et al.*, Phys. Rev. C **52**, 604 (1995).

[14] F. Ajzenberg-Selove, Nucl. Phys. **A506**, 1 (1990).

[15] J. Raynal, program DWBA98, 1209/05, NEA (1999).

[16] H. Fujimura *et al.*, Phys. Rev. C **69**, 064327 (2004).

[17] S. van der Werf, S. Brandenburg, P. Grasduk, W. Sterrenburg, M. Harakeh, M. Greenfield, B. Brown, and M. Fujiwara, Nucl. Phys. **A496**, 305 (1989).

[18] S. Cohen and D. Kurath, Nucl. Phys. **73**, 1 (1965).

[19] Y. Fujita *et al.*, Phys. Rev. C **67**, 064312 (2003).

[20] M. A. Franey and W. G. Love, Phys. Rev. C **31**, 488 (1985).

[21] T. Taddeucci *et al.* Phys. Rev. C **42**, 935 (1990).

[22] T. Taddeucci, C. Goulding, T. Carey, R. Byrd, C. Goodman, C. Gaarde, J. Larsen, D. Horen, J. Rapaport, and E. Sugarbaker, Nucl. Phys. **A469**, 125 (1987).

[23] Y. Satou *et al.*, Phys. Lett. B **549**, 307 (2002).

[24] J. Raynal, program ECIS95, 0850-14, NEA (1995).

[25] G. Satchler, *Direct Nuclear Reactions* (Oxford University Press, New York, 1983).

[26] S. Hama, B. Clark, E. Cooper, H. Sherif, and R. Mercer, Phys. Rev. C **41**, 2737 (1990).

[27] V. Hannen *et al.*, Phys. Rev. C **67**, 054321 (2003).

[28] T. Suzuki, R. Fujimoto, and T. Otsuka, Phys. Rev. C **67**, 044302 (2003).

[29] R. Raghavan and S. Pakvasa, Phys. Rev. D **37**, 849 (1988).